T-P-LB-3597

Diet-Induced Intestinal Mucosal Disequilibrium Contributes to Insulin-Resistant Metabolic Disease

Jason A. West, PhD[1]; Anastasia Tsakmaki, PhD[2]; Jason H.S. Huang, MS[1]; Soumitra S. Ghosh, PhD[3]; David G. Parkes, PhD[4]; Pernille Wismann, PhD[5]; Kristoffer T.G. Rigbolt[5]; Philip J. Pedersen, DVM, PhD[5]; Polychronis Pavlidis[6]; David Maggs, MD[1]*; Juan Carlos Lopez-Talavera, MD, PhD[1]; Gavin A. Bewick, PhD[2]; Harith Rajagopalan, MD, PhD[1]

[1]Fractyl Laboratories Inc, Lexington, MA, USA; [2]Diabetes Research Group, School of Life Course Sciences, Faculty of Life Science and Medicine, King's College London, London, UK; [3]Doon Associates, San Diego, CA, USA; [4]DGP Scientific Inc, San Diego, CA, USA; [5]Gubra ApS, Hørsholm, Denmark; [6]Centre for Inflammation Biology and Cancer Immunology, King's College London, London, UK. *Currently employed by Becton Dickinson Technologies & Innovation, Raleigh-Durham, NC, USA

Background

- Excessive consumption of diets high in saturated and trans fats and refined sugar is one of the primary drivers of insulin resistance and hyperinsulinemia that underlie obesity and metabolic diseases[1–2]
- Gastrointestinal procedures (eg, bariatric/metabolic surgery) that bypass the upper small intestine (eg, Roux-en-Y gastric bypass [RYGB] surgery, duodenal-jejunal bypass) induce dramatic and long-lasting weight-independent improvements in glycemic control, lipid metabolism, inflammation, and insulin resistance in patients with type 2 diabetes (T2D),[3] highlighting the important role of the gut as a critical regulator of metabolic homeostasis[4–14]
- The gut epithelium dynamically responds to local nutrient exposure, and each gut region exhibits distinct mucosal physiology[15–18]
- Fundamental questions regarding the relative contributions of factors produced by the proximal and distal small intestine—and the potential for a causal role of intestinal mucosal changes in obesity and the dysmetabolic state—remain unanswered
- Understanding the mechanisms by which bypass of the duodenum and/or nutrient delivery to the distal bowel leads to lasting improvements in metabolic homeostasis provides an opportunity to refine current treatments and develop new therapies for metabolic diseases[19]

Objective

To further elucidate the potential mechanisms underlying nutrient-induced gut adaptation and insulin resistance–related metabolic disease pathogenesis, we report key findings that highlight the important and distinct contributions of the proximal and distal intestinal mucosa in regulating metabolic homeostasis.

Methods

- To further characterize nutrient-induced gut adaptation we studied:
  - Intestinal changes in morphology, hormonal signaling, and transcription in high-fat diet (HFD)–induced obese mice
  - Effects of direct stimulation with lipid or glucose on proximal and distal intestinal epithelial growth using rodent and human organoids
- To investigate the pathophysiologic relevance of nutrient-induced gut adaptation, we studied the effect of:
  - Surgical intervention (RYGB) on proximal and distal intestinal morphology and gene expression in diet-induced obese (DIO) rats
  - Pharmacologic manipulation of proximal (glucose-dependent insulinotropic polypeptide [GIP]) and distal (glucagon-like peptide-1 [GLP-1]) gut hormones on glucose and lipid metabolism in DIO rodents

HFD-induced obese (DIO) mice

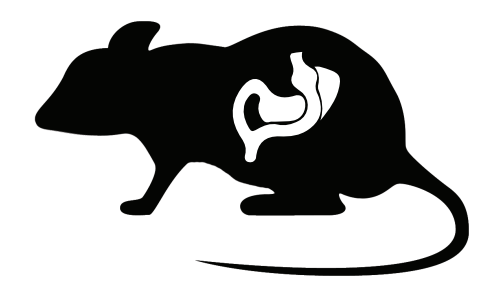

RYGB in DIO rats

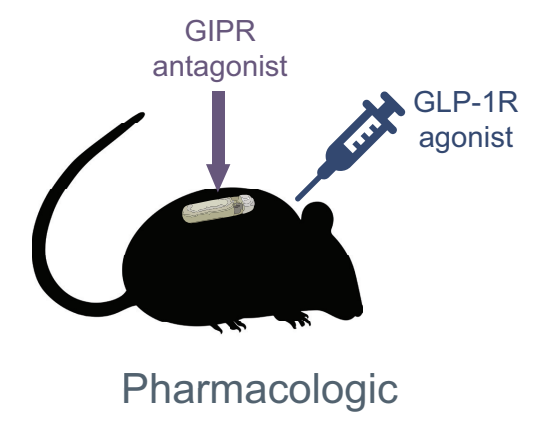

Pharmacologic GIPR Antagonism ± GLP-1R Agonists in DIO mice

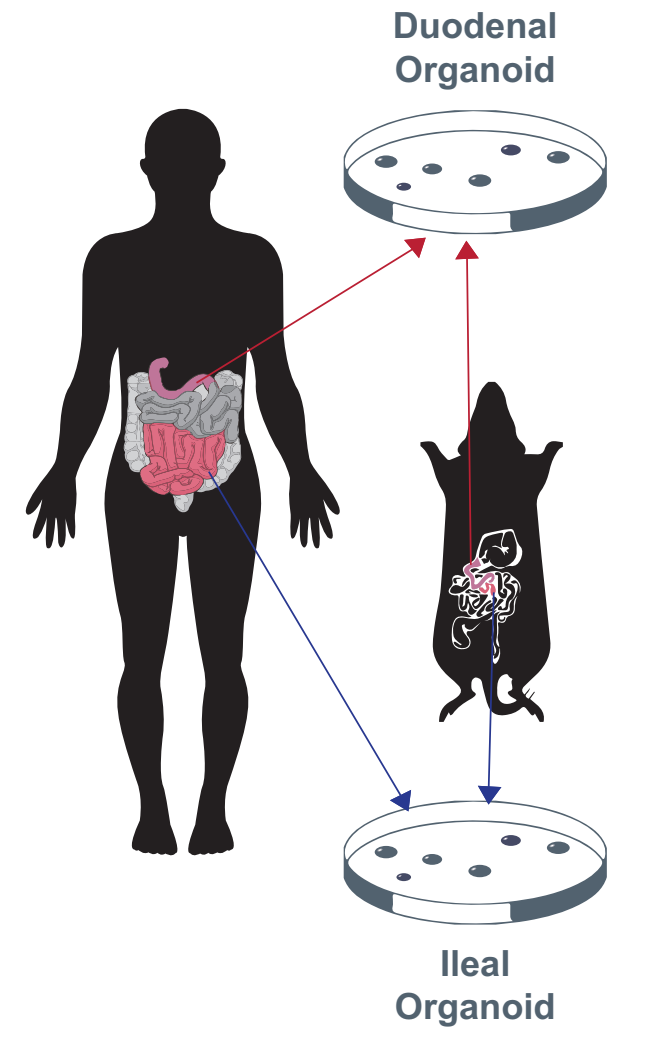

High-fat Diet-induced Obesity Mouse Model

- C57Bl/6JRj mice were fed lean chow (11% fat, 24% protein, 65% carbohydrate) or HFD (60% fat, 20% protein, 20% carbohydrate) for 7 or 13 weeks

RYGB in DIO Rat Model

- Sprague Dawley rats were fed a 2-choice diet of HFD (29.3% fat, 33.2% carbohydrate, and 18% protein) and pelleted chow *ad libitum* for 20 weeks and were randomized 1:3 to receive RYGB or sham surgical procedure
- Post-procedure, rats were fed a liquid diet (fat 3.4%, carbohydrate 13.8%, and protein 3.8%) from day –3 to day 11, then HFD and chow or chow only from days 11 to 21 (study termination)

GIP Receptor Antagonism Combined with GLP-1 Receptor Agonism in DIO Mouse

- C57BL/6JRj mice were fed a HFD for 18 weeks before and during the study
- Mice received treatment from day 0 (first dose) through day 28
  1. **Vehicle:** Vehicle 1 (phosphate buffered saline plus 0.1% bovine serum albumin, subcutaneous [SC], once daily [QD]) and continuous infusion of vehicle 2 (DMSO/propylene glycol [50/50 v/v]) via osmotic minipump
  2. **GLP-1 receptor (GLP-1R) agonist:** 0.2 mg/kg liraglutide and continuous infusion of vehicle 2 via osmotic minipump
  3. **GIP receptor (GIPR) antagonist:** Vehicle 1 (SC, QD) and continuous infusion of ~4.5 mg/kg/day mouse GIP(3-30)NH2[16] via osmotic minipump
  4. **GLP-1R agonist + GIPR antagonist:** 0.2 mg/kg liraglutide (SC, QD) and continuous infusion of ~4.5 mg/kg/day mouse GIP(3-30)NH2 via osmotic minipump

Human and Mouse Intestinal Organoids

- Mouse duodenal and terminal ileum crypts were isolated and grown into organoids as previously described[9]
- Human duodenal and terminal ileum crypts were isolated from biopsy samples taken from 2 different patients undergoing endoscopy at Guy's and St Thomas' NHS Foundation Trust
  - Crypts from those biopsy samples were isolated and grown into organoids as previously described[10]

Results

HFD Results in Opposite Effects on Intestinal Growth and Metabolism in the Proximal vs Distal Gut

- HFD causes mucosal hyperplasia in the proximal gut (the duodenum and the upper jejunum), while the distal gut (ileum and colon) showed hypoplasia **(Figure 1)**
  - Mean GLP-1–positive cell number ($P < 0.01$), *Glp* transcription ($P < 0.05$), and crypt density ($P < 0.001$) were greater in the duodenum and jejunum of DIO mice compared with control mice, suggesting an adaptive growth response by the stem cell compartment
  - HFD also altered hormone expression across segments of the gut commensurate with the changes in mucosal thickness
- Pathway analyses on RNA-sequencing data indicated a robust impact of diet on gut hormone production, cholesterol homeostasis/ketogenesis, glycolysis, fatty acid metabolism, oxidative phosphorylation, and immune response **(Figure 2)**
  - The proximal gut showed significant changes in gene expression in response to DIO for many genes from these pathways, while, in general, their expression was not markedly impacted in distal segments of the intestine

Figure 1. HFD-induced Adaptive Responses in Mouse Intestinal Mucosa, Enteroendocrine Cell Numbers, and Transcriptional Changes in Gut Hormones

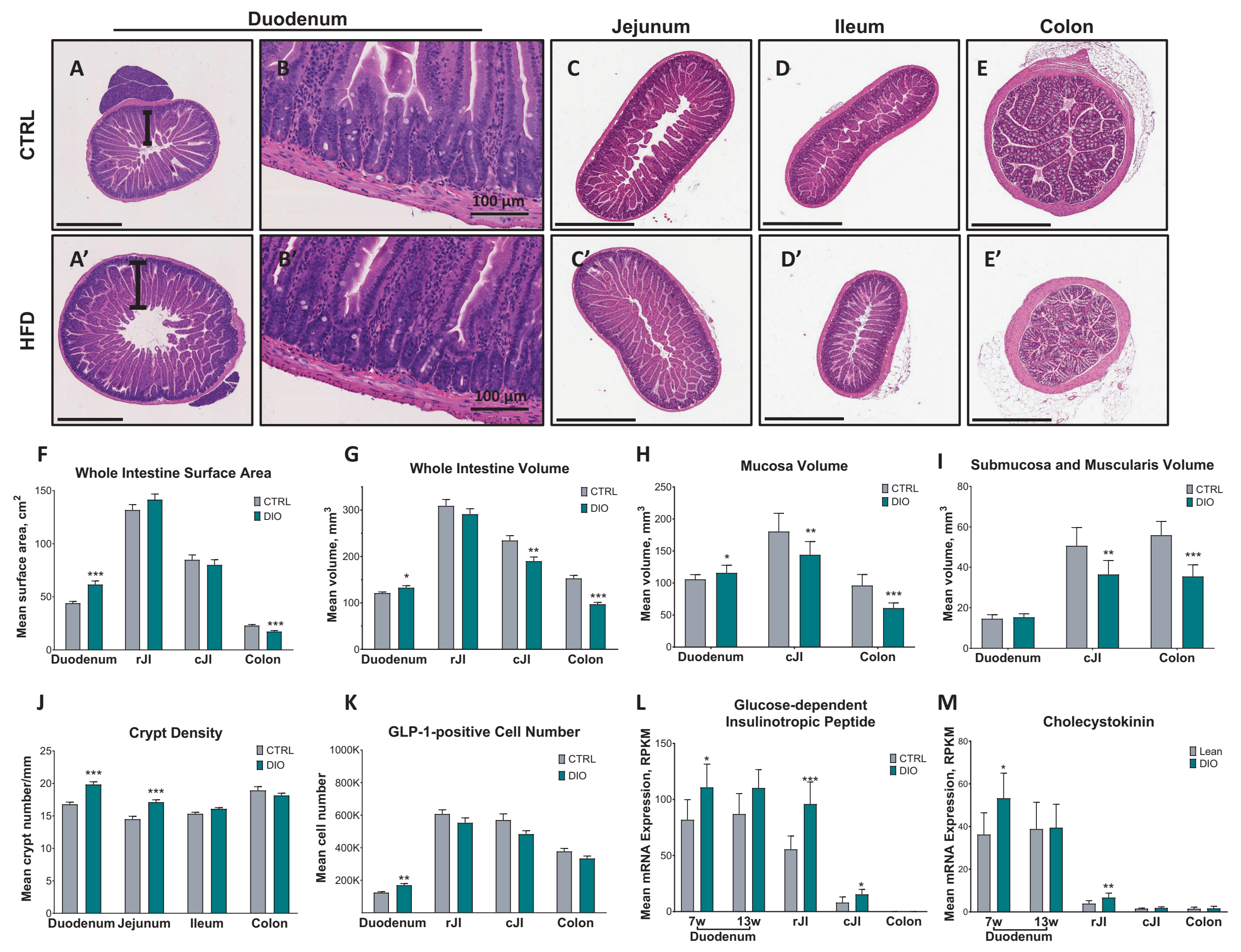

Representative hematoxylin and eosin–stained cross-sections of duodenum, jejunum, ileum, and colon from mice fed lean chow (CTRL) (A–E) or HFD (A'–E'). Scale bar = 1000 µm, unless otherwise noted. The mucosal layer is bracketed in panels A and A'. Whole intestine surface area in cm² (F), whole intestine volume in mm³ (G), mucosa volume in mm³ (H), and submucosa and muscularis volume in mm³ (I) estimated by stereology in mice following consumption of CTRL chow or HFD (DIO) for 13 weeks by intestinal region. (J) Histological quantification of crypt density (number/mm) in DIO and CTRL groups at 13 weeks. Whole intestine *Glp-1*–positive cell number (K) by intestinal region in CTRL or DIO mice at 13 weeks. mRNA expression levels of *Gip* (L) and *Cck* (M) by intestinal region (13-week data presented for rJI, cJI, and colon regions). Data are presented as mean ± SEM. Statistical significance was evaluated using unpaired *t* test with $***P < 0.001$, $**P < 0.01$, and $*P < 0.05$. cJI = caudal jejunoileum; *Cck* = cholecystokinin; CTRL = control; DIO = diet-induced obesity; *Gip* = glucose-dependent insulinotropic polypeptide; *Glp-1* = glucagon-like peptide-1; HFD = high-fat diet; rJI = rostral jejunoileum; RPKM = reads per kilobase per million sequence reads; SEM = standard error of the mean.

Figure 2. HFD-induced Expression Changes in Metabolic and Immune Response Pathways

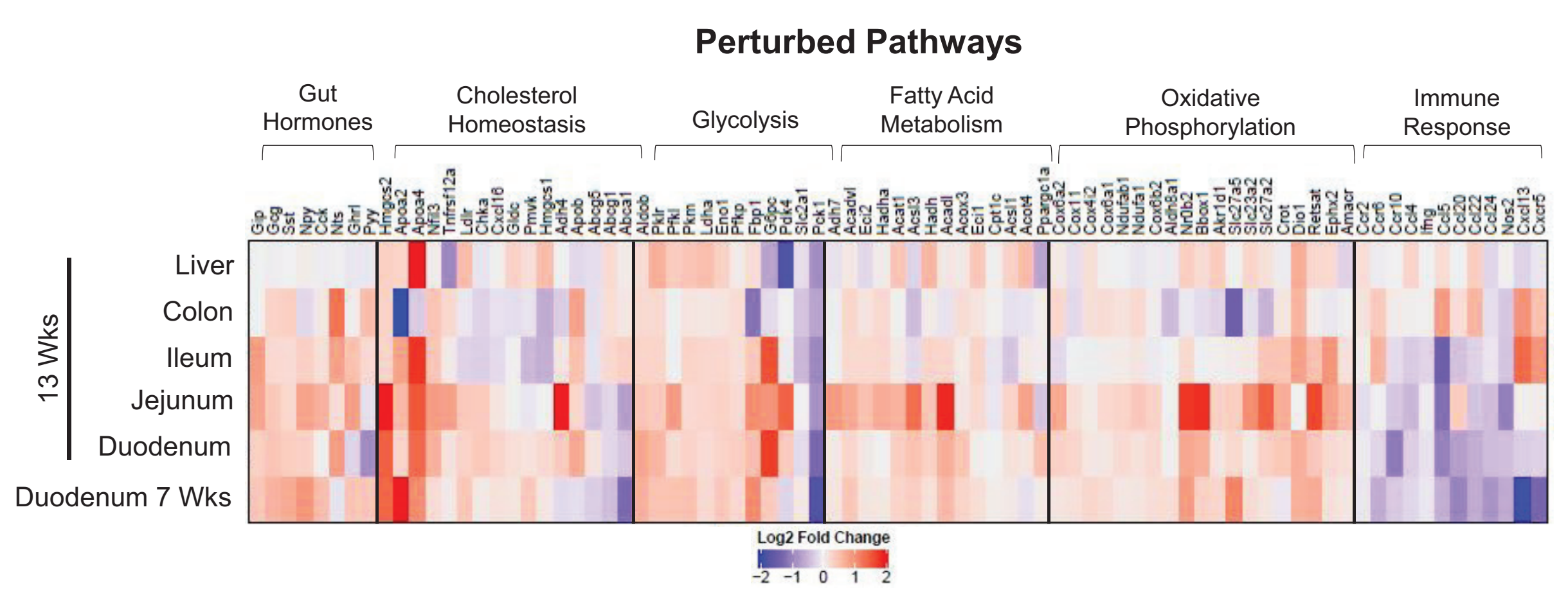

Heat map of mean $\log_2$-fold change in expression levels of genes linked to pathways perturbed by a HFD vs lean chow (control) in samples from duodenum at 7 weeks and from duodenum, jejunum, ileum, colon, and liver at 13 weeks post-initiation of dietary intervention. Pathway (gene sets of HallMarks/KEGG pathways) expression in the duodenum at 7 weeks (n = 10), and duodenum (n = 10), jejunum/rJI (n = 8), ileum/cJI (n = 6), colon (n = 8), and liver (n = 8) at 13 weeks was compared between mice fed with a HFD or control with an adjusted FDR *P* value (q value) < 0.25 considered significant. A statistically significant impact of diet was found in the rJI for gene pathways related to fatty acid metabolism, oxidative phosphorylation, glycolysis/gluconeogenesis, and bile acid metabolism. cJL = caudal jejunoileum; HFD = high-fat diet; FDR = false discovery rate; KEGG = Kyoto encyclopedia of genes and genomes; rJI = rostral jejunoileum.

Nutrient Exposure Produces Differential Response in Duodenal vs Ileal Organoids

- Transcriptional responses diverged between mouse duodenal and ileal organoids in response to chronic exposure to excess lipid **(Figure 3)**
- Results from human organoid experiments demonstrated that the duodenal and ileal stem cell compartments differentially respond to excess nutrients (either lipid or glucose) *in vitro* **(Figure 4)**, supporting the observations of duodenal hyperplasia and ileal hypoplasia seen after DIO in rodents *in vivo*

Figure 3. Distinct Changes in Gene Expression of Mouse Duodenal and Ileal Organoids After Chronic Exposure to Lipids

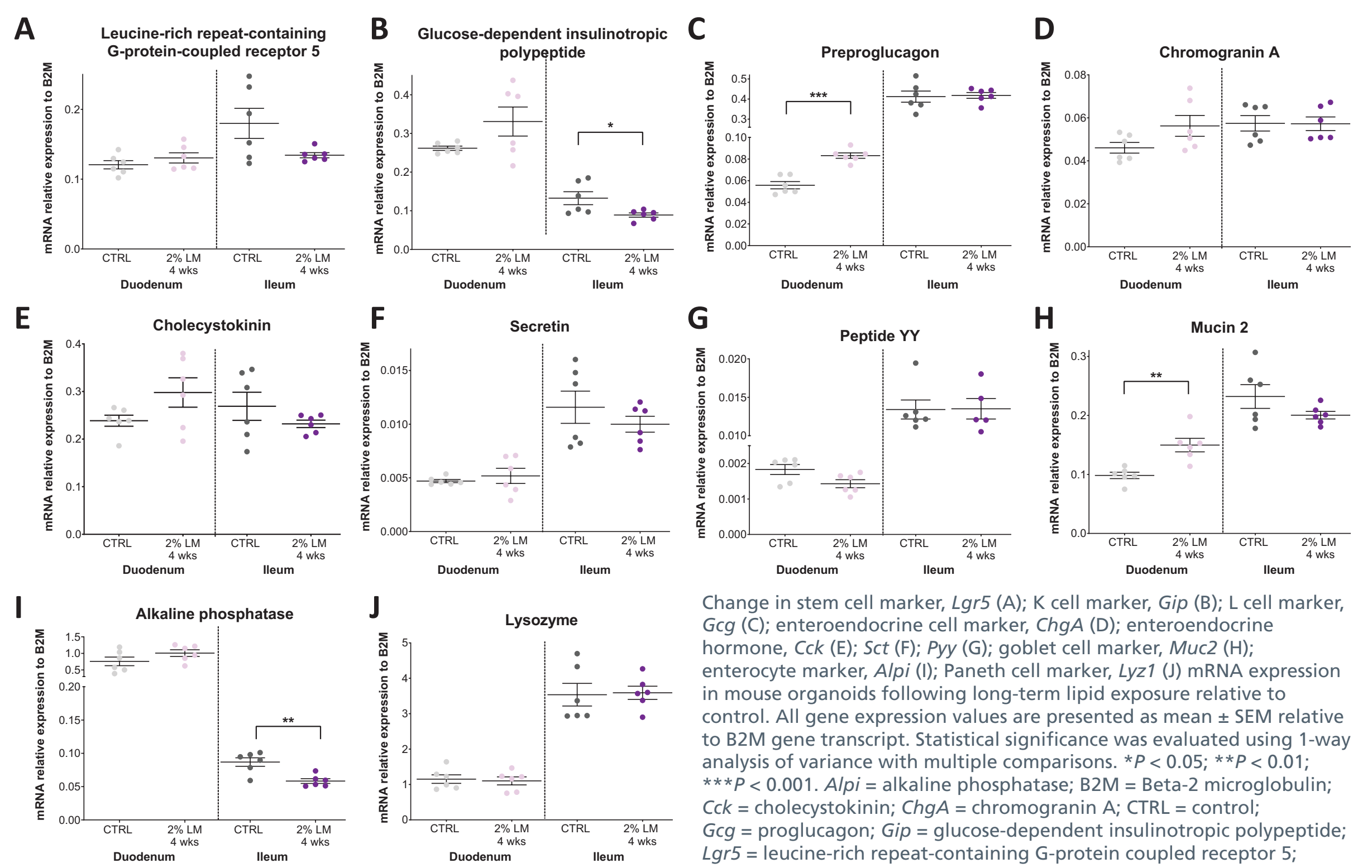

Change in stem cell marker, *Lgr5* (A); K cell marker, *Gip* (B); L cell marker, *Gcg* (C); enteroendocrine cell marker, *ChgA* (D); enteroendocrine hormone, *Cck* (E); *Sct* (F); *Pyy* (G); goblet cell marker, *Muc2* (H); enterocyte marker, *Alpi* (I); Paneth cell marker, *Lyz1* (J) mRNA expression in mouse organoids following long-term lipid exposure relative to control. All gene expression values are presented as mean ± SEM relative to B2M gene transcript. Statistical significance was evaluated using 1-way analysis of variance with multiple comparisons. $*P < 0.05$; $**P < 0.01$; $***P < 0.001$. *Alpi* = alkaline phosphatase; B2M = Beta-2 microglobulin; *Cck* = cholecystokinin; *ChgA* = chromogranin A; CTRL = control; *Gcg* = proglucagon; *Gip* = glucose-dependent insulinotropic polypeptide; *Lgr5* = leucine-rich repeat-containing G-protein coupled receptor 5; LM = lipid mixture; *Lyz1* = lysozyme; *Muc2* = mucin 2; *Pyy* = peptide YY; *Sct* = secretin; SEM = standard error of the mean.

Figure 4. Divergent Growth and Transcriptional Responses of Human Duodenal and Ileal Organoids to Lipid and Glucose Treatment

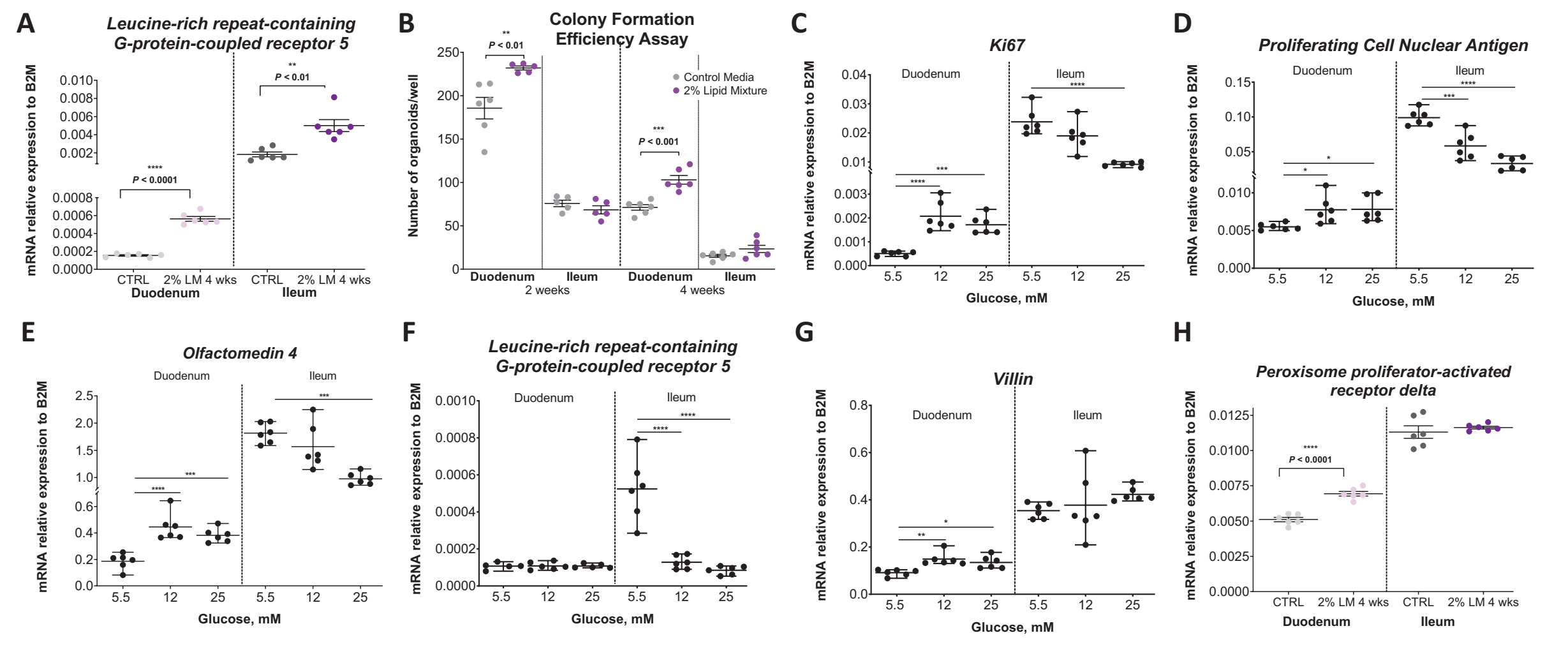

(A) *LGR5* expression in human duodenal and ileal organoids after 4 weeks of 2% lipid exposure. (B) Organoid colony formation efficiency assays performed at weeks 2 and 4 of 2% lipid exposure revealed significantly increased stemness in duodenal but not in ileal organoids. Impact of exposure of human duodenal and ileal organoids to increased concentrations of glucose (5.5 mM, 12 mM, and 25 mM) on mRNA expression levels of *Ki67* (C); *PCNA* (D); *OLFM4* (E); *LGR5* (F); and villin (G). *PPAR-d* expression in human duodenal and ileal organoids after 4 weeks of 2% lipid exposure (H). All gene expression values are presented relative to B2M gene transcript. Data are plotted as mean ± standard error of the mean. Statistical significance in lipid mixture experiments was evaluated using unpaired *t* test and in glucose experiments using 1-way ANOVA with $*P < 0.05$; $**P < 0.01$; $***P < 0.001$; $****P < 0.0001$. ANOVA = analysis of variance; B2M = beta-2-microglobulin; CTRL = control; *LGR5* = leucine-rich, repeat-containing G-protein-coupled receptor 5; LM = lipid mixture; *OLFM4* = olfactomedin 4; *PPAR-d* = peroxisome proliferator-activated receptor-delta; *PCNA* = proliferating cell nuclear antigen; wks = weeks.

RYGB Surgery Elicits Morphologic and Hormonal Changes to Proximal vs Distal Intestine that Oppose Changes Seen in DIO Models

- HFD induced distinct changes to proximal and distal gut, and RYGB-directed nutrient exposure to the distal gut led to opposing adaptive morphological and gene expression changes that correlated with metabolic benefit **(Figure 5)**
  - 3 weeks post-procedure, there was a significant increase in distal ($P < 0.001$) jejunum weight **(Figure 5B)** and proximal ($P < 0.01$) and distal ($P < 0.001$) jejunum volume **(Figure 5C)** in DIO-RYGB rats compared with sham-operated DIO rats
  - Immunohistochemistry analysis indicated that GIP cell density was reduced after RYGB in the alimentary and common limb
  - The mean expression of other proximal intestinal gut hormones (including Gip, Cck, and ghrelin and obestatin prepropeptide [Ghrl]) were significantly downregulated following RYGB in the duodenum compared with a sham procedure ($P < 0.001$, $P < 0.05$, and $P < 0.01$, respectively), contrasting to the increase in GIP expression seen following HFD in sham-operated DIO rats
- Similar to DIO mouse gene expression data, we noted a marked impact of HFD on the expression of genes responsible for gut hormone production, cholesterol homeostasis, glycolysis, and fatty acid and bile acid metabolism in the proximal gut, including the duodenum and jejunum **(Figure 6)**
  - RYGB often demonstrated opposite effects on gene expression when compared with the DIO-sham procedure
  - HFD-induced increases in expression of proximal gut hormones and genes involved in fatty acid and bile acid metabolism were countered by large reductions in expression of these genes in the proximal gut after RYGB

Figure 5. RYGB Surgery in DIO Rat Model Establishes the Importance of the Proximal and Distal Gut Morphology and Gene Expression

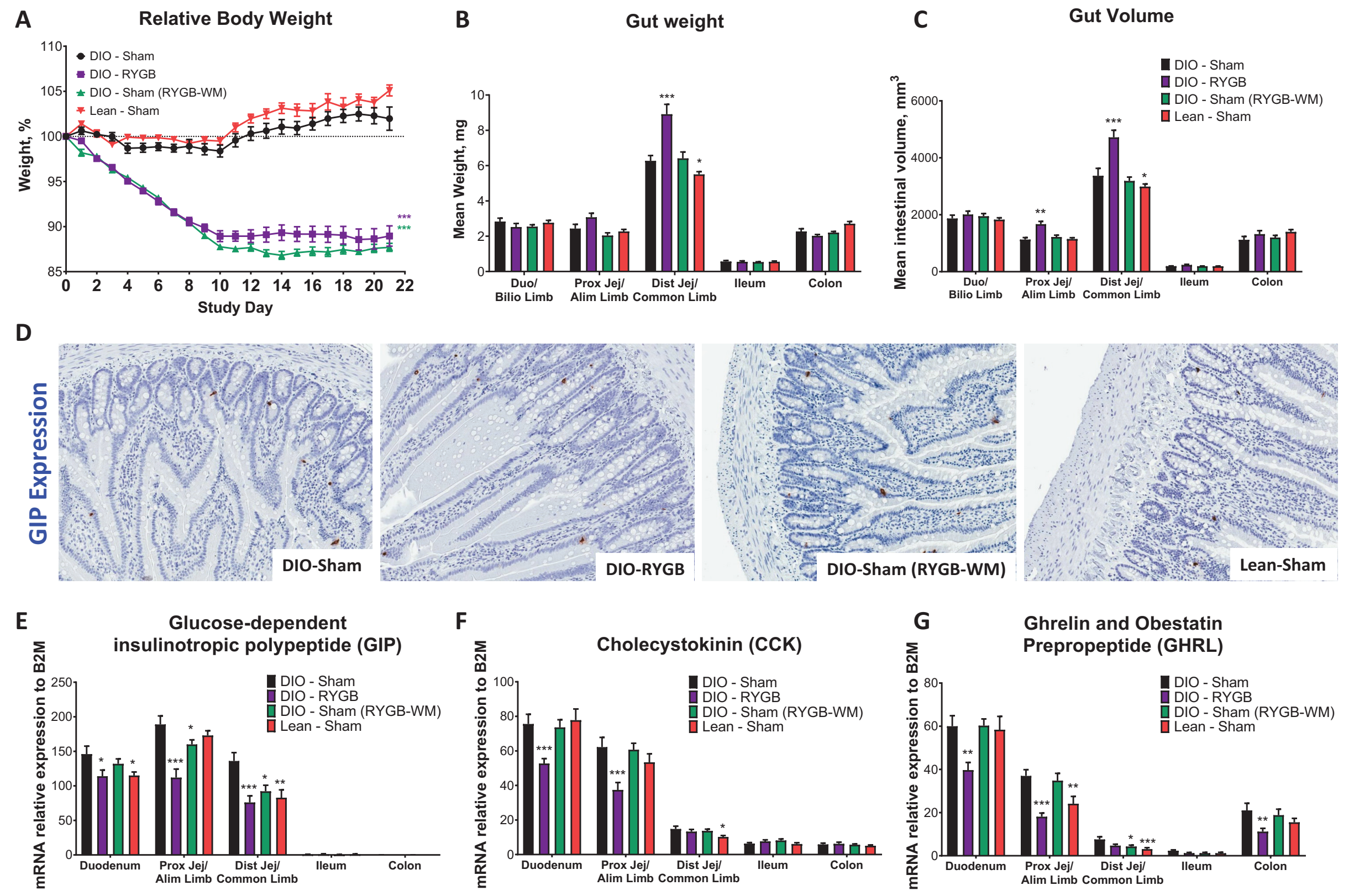

(A) Relative body weight from day 0 to 21. (B) Gut weight (milligrams) by region. (C) Gut volume (millimeters) by region. (D) Representative images of GIP immunohistochemistry in duodenum/bibliopancreatic limb (magnification 10×). *Gip* (E), *Cck* (F), and *Ghrl* (G) mRNA expression levels by gut region. Data are presented as mean (SEM), unless otherwise noted. Significant differences between treatment groups were determined using Dunnett's test 1-factor (total body weight, total gut weight and volume, mucosal weight) linear model of last study day data or 2-factor (intestinal weight and volume in different intestinal regions) linear model with interaction. $*P < 0.05$; $**P < 0.01$; $***P < 0.001$ after correction for gene-wise multiple testing. N = 10 for each group. *Cck* = cholecystokinin; *Ghrl* = ghrelin and obestatin prepropeptide; *Gip* = glucose-dependent insulinotropic polypeptide; RYGB = Roux-en-Y gastric bypass; SEM = standard error of the mean.

Figure 6. RYGB Affects the Gene Expression in Metabolic Regulation Pathways Distinctly in Proximal vs Distal Segments of the Intestine

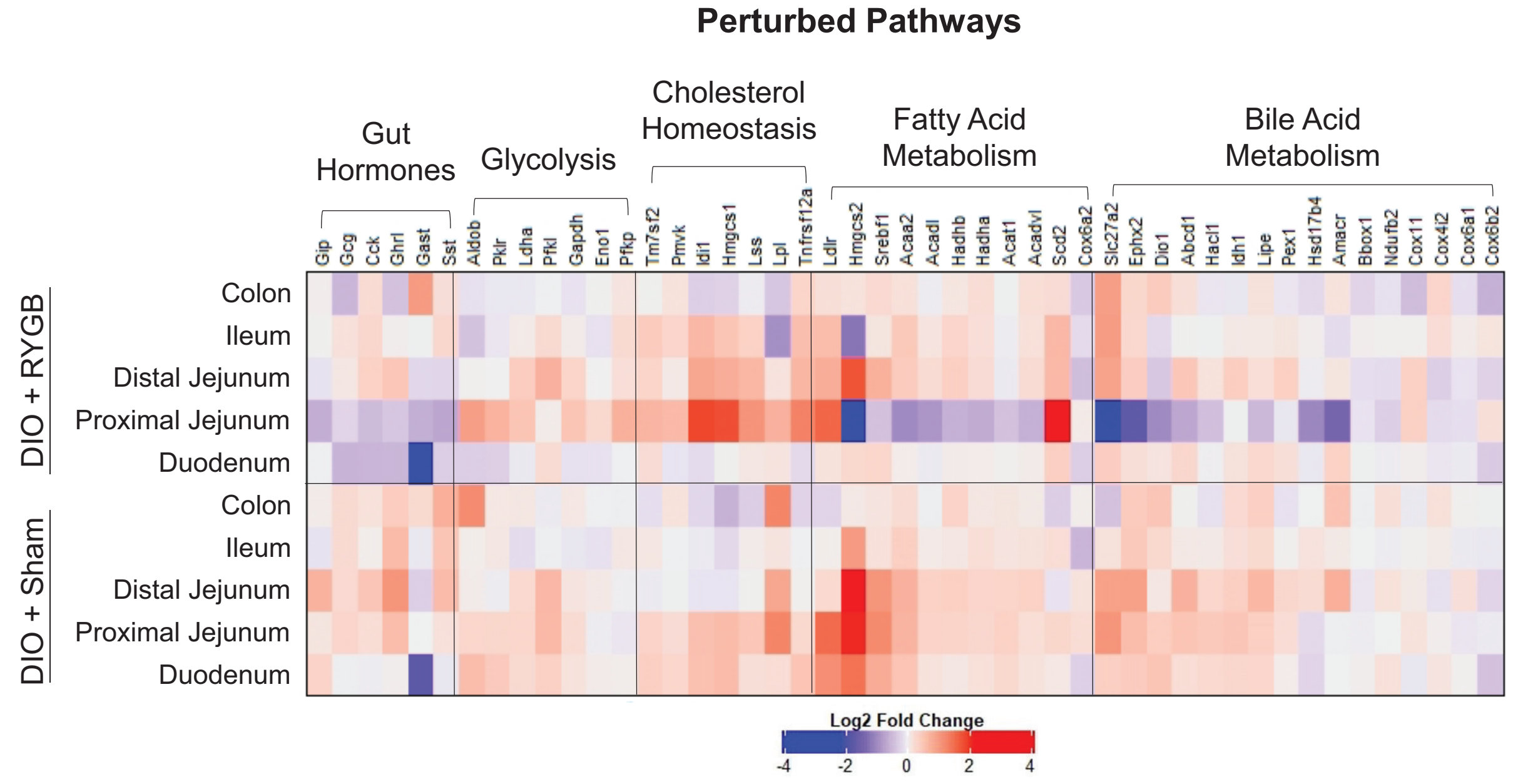

Heat map of mean $\log_2$-fold change expression levels of genes linked to pathways found to be perturbed by either DIO-sham procedure or DIO-RYGB vs lean-sham controls (adjusted FDR $P < 0.25$ considered significant). A statistically significant impact of RYGB was found in the proximal jejunum for gene pathways–related cholesterol homeostasis. Labeling was simplified based on the following: Duodenum for both duodenum in sham control animals or biliopancreatic limb after RYGB, proximal jejunum for both proximal jejunum in sham-controlled animals, and alimentary limb after RYGB, proximal jejunum for both proximal jejunum in sham animals, and common channel after RYGB. DIO = diet-induced obesity; FDR = false discovery rate; RYGB = Roux-en-Y gastric bypass. N = 10 for each group.

DISCLOSURES

SSG has received honorarium for consultancy from Fractyl Laboratories Inc. **AT** has received funding/grant support from JDRF. **PW, KTGR,** and **PJP** are employees of Gubra ApS. **DGP** has received honorarium for consultancy from Fractyl Laboratories Inc. **PP** has received funding/grant support from CCUK, GutsUK, King's Health Partners, and the Rosetrees Trust. **DM** is a former employee of Fractyl Laboratories Inc. He is a current shareholder, and has received honorarium for consultant activities from Fractyl Laboratories Inc. **HR, JAW, JCLT,** and **JHSH** are employees and shareholders of Fractyl Laboratories Inc. **GAB** has received funding/grant support from EFSD and JDRF and honorarium for consultant activities from Fractyl laboratories Inc.

ACKNOWLEDGMENTS

Supported by funding from Fractyl Laboratories Inc. The authors would like to thank Prof Francesco Rubino for his contributions to these studies and his thoughtful review and helpful insight on the poster. Editorial assistance, funded by Fractyl Laboratories Inc, provided by Caroline W Cazares, PhD, of JB Ashtin.

REFERENCES

1. Cordain L, et al. *Am J Clin Nutr*. 2005;81:341–354; 2. Danaei G, et al. *Circulation*. 2013;127:1493–1502, 1502e1491–1498; 3. Rubino F, et al. *Diabetes Care*. 2016;39:861–877; 4. Mingrone G, et al. *N Engl J Med*. 2012;366:1577–1585; 5. Ferrannini E, et al. *Diabetes Care*. 2009;32:514–520; 6. Salinari S, et al. *Am J Physiol Endocrinol Metab*. 2013;305:E59–66; 7. Zervos EE, et al. *J Am Coll Surg*. 2010;210:564–572; 8. Rubino F, et al. *Ann Surg*. 2004;240:236–242; 9. Rubino F, et al. *Ann Surg*. 2006;244:741–749; 10. Umeda LM, et al., *Obes Surg*. 2011;21:896–901; 11. Dirksen C, et al., *Diabetes Care*. 2010;33:375–377; 12. Cummings DE, et al., *Surg Obes Relat Dis*. 2007;3:109–115; 13. Laursen TL, et al. *WJH*. 2019;27:138–149; 14. Jirapinyo P, et al. *Diabetes Care*. 2018;41:1106–1115; 15. Sandoval D. *Gastroenterology*. 2016;150:309–312; 16. de Wit NJ, et al. *BMC Med Genomics*. 2008;1:14; 17. Gerhart H, et al. *Cell*. 2019;176:1158–1173; 18. Reimann and Gribble *JDI*. 2016;7:13–19; 19. de Jonge C, et al. *Obes Surg*. 2013;23:1354–1360.

Effect of GIP Receptor Antagonism Combined with GLP-1 Receptor Agonism on Metabolic Control in DIO Mice

- Differential perturbation of gut hormonal signals from the proximal and distal gut may have mutually reinforcing effects on metabolic homeostasis **(Figure 7)**
  - Mice treated with the GIPR antagonist in combination with the GLP-1R agonist had lower epididymal fat weight at termination than mice treated with the GLP-1R agonist alone
  - Pharmacologic inhibition of the duodenal hormone GIP, together with GLP-1R agonism, reduces HFD-induced hyperinsulinemia and insulin resistance

Figure 7. The Effect of GIPR Antagonism Via GIP(3-30)NH2 in Combination With Liraglutide on Glucose and Lipid Homeostasis in DIO Mice

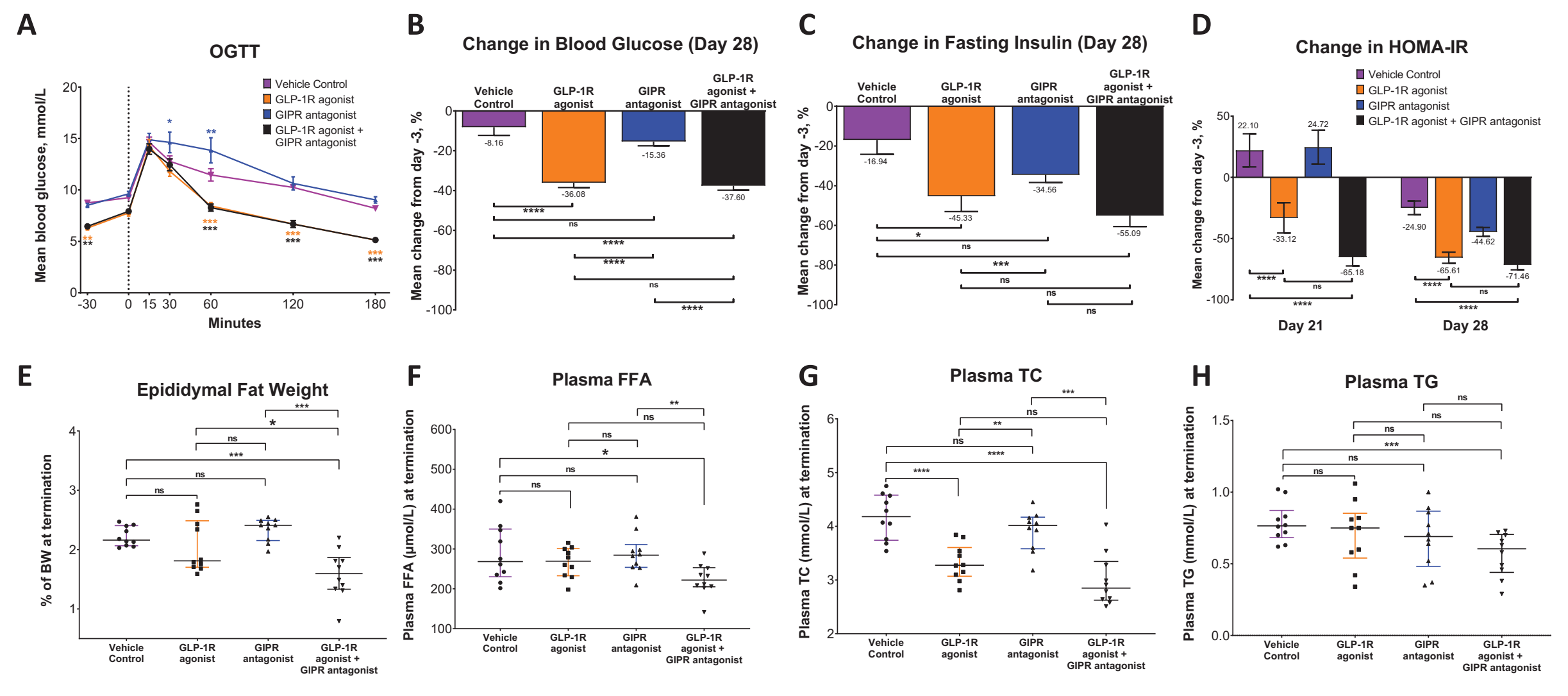

(A) Blood glucose (millimoles per liter) during the OGTT on day 21 measured at –30, 0, 15, 30, 60, 120, and 180 minutes relative to oral glucose load. Animals were dosed at –30 minutes. (B) Percent change in blood glucose from day –3 to day 28. (C) Percent change from day –3 to day 28 in fasting insulin. (D) Percent change in HOMA-IR from day –3 to day 21 and from day –3 to day 28. (E) Mean (interquartile range) terminal epididymal fat weight relative to body weight. (F) Mean (interquartile range) plasma FFAs (micromoles per liter) at termination. (G) Median (interquartile range) of plasma TC (millimoles per liter) at termination. (H) Median (interquartile range) of plasma TG (millimoles per liter) at termination. Data are presented as mean ± SEM, unless otherwise noted. For continuous data from minipump experiments with a single time point or repeated measures, a 1-factor linear model was used to compare difference in plasma insulin, TG, TC, FFA, and epididymal fat weight between treatments and control using Dunnett's test. A 2 × 2 contingency table consisting of responders and non-responders in control and treatment groups was used to analyze categorical data, and a Fisher's exact test was used for all pairwise comparisons with *P* values adjusted using the Bonferroni correction. $*P < 0.05$; $**P < 0.01$; $***P < 0.001$ compared with vehicle. FFA = free fatty acid; GIPR = glucose-dependent insulinotropic polypeptide receptor; GLP-1R = glucagon-like peptide-1 receptor; HOMA-IR = homeostatic model assessment-insulin resistance; OGTT = oral glucose tolerance test; SEM = standard error of the mean; TC = total cholesterol; TG = triglycerides. N = 10 for each group.

Summary Of Key Findings

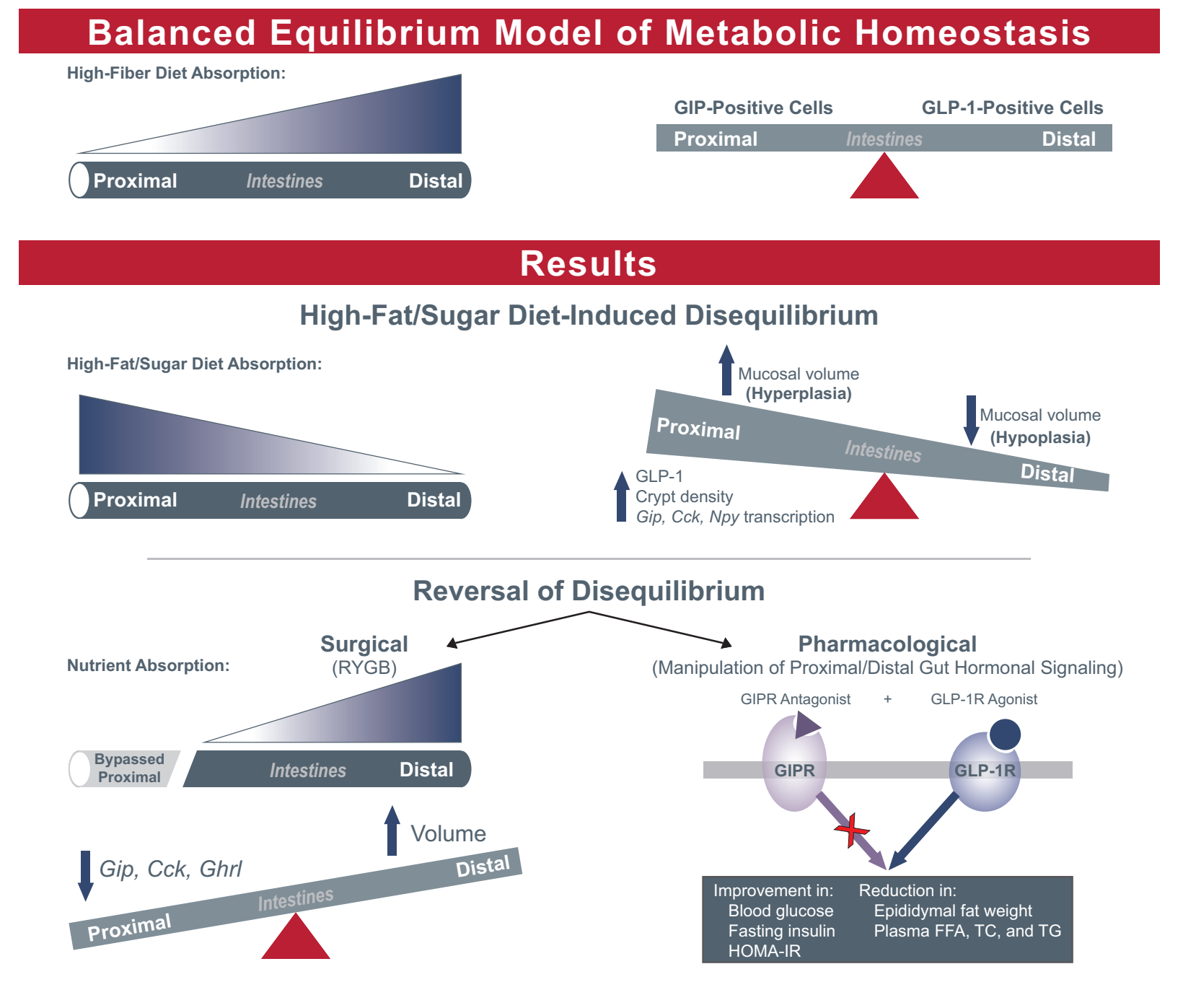

Figure 8. Nutrients differentially impact the proximal and distal gut, which leads us to propose a balanced equilibrium model of the intestinal mucosa's influence on metabolic homeostasis and IR-related disease pathogenesis. We hypothesize that HFD-induced duodenal hyperplasia, accompanied by ileal hypoplasia, results in metabolic imbalance between proximal gut signals (eg, enteroendocrine function) vs distal gut signals that together contribute to a dysmetabolic state (eg, insulin resistance) in humans. Although regional-specific gut hormones play an important role in our balanced equilibrium model, other factors such as lipid metabolism, neuronal signaling, microbiome effects, and bile acid signaling, are also important contributors. GLP-1 indicates an increase in the number of GLP-1–positive cells. *Cck* = cholecystokinin; *Ghrl* = ghrelin and obestatin prepropeptide; *Gip* = glucose-dependent insulinotropic polypeptide; GIPR = GIP receptor; GLP-1 = glucagon-like peptide-1; GLP-1R = GLP-1 receptor; HOMA-IR = homeostatic model assessment-insulin resistance; TC = total cholesterol; TG = triglycerides; RYGB = Roux-en-Y gastric bypass.

Conclusions

- **Diet with a high content of fat and sugar induces distinct and opposite effects in the growth and metabolism of the proximal vs distal gut**
- **Morphologic and functional imbalance between the proximal and distal intestine is associated with a dysmetabolic phenotype**
- **Improved metabolic function after surgical and pharmacological intervention is associated with restored balance between proximal and distal intestine**
- **These findings (Figure 8) further support the role of the intestinal epithelium in the control of metabolism and suggest that interventions aimed at maintaining or restoring physiological balance between the proximal and the distal intestine may be effective ways to prevent and treat T2D and other metabolic diseases**

Obesity Week 2019 | November 3–7, 2019 | Las Vegas, NV

FRACTYL